Appl Phys A (2011) 105:69–74
DOI 10.1007/s00339-011-6526-6

Applied Physics A
Materials Science & Processing

Evolution of hole depth and shape in ultrashort pulse deep drilling in silicon

S. Döring · S. Richter · A. Tünnermann · S. Nolte

Received: 9 May 2011 / Accepted: 1 July 2011 / Published online: 29 July 2011

Abstract We report on the temporal evolution of the percussion drilling process in deep laser drilling. Ultrashort laser pulses at 1030 nm and a duration of 8 ps were used to machine silicon while simultaneously imaging the silhouette of the hole using an illumination wavelength above the band edge. We investigate the influence of the processing parameters fluence and pulse energy on the depth and shape of the hole demonstrating different phases of the drilling process. In the first phase, a tapered hole is formed with highly reproducible shape and depth. In the following, the evolution of the hole shape is irregular and imperfections like bulges, changes of the drilling direction and the formation of multiple hole ends occur. In the final phase, the maximum depth stays constant while the volume still increases due to enlargement of the hole diameter and the possible formation of multiple hole ends. Deviations from the ideal hole shape occur primarily in the lower part of the hole. Their extent can be reduced by increasing the amount of applied pulse energy. Moreover, the pulse energy is chiefly determining the maximum achievable hole depth, which is largely independent of the focusing conditions and corresponding fluence.

1 Introduction

The use of ultrashort laser pulses in materials processing offers the possibility of high quality, high precision manufacturing on a micrometer scale. Therefore, the laser material interaction is of fundamental interest for process optimization and control. Prior studies covered the influence of the principal laser parameters like pulse duration, fluence, and pulse energy [1, 2]. For a given pulse duration, the fluence determines the ablation rate on the surface [3, 4]. In addition, the generated plasma and particles have been studied to gain insight in the physics of the ablation mechanism [5–7]. However, in most cases, these investigations were limited to the surface. For deep structures with high aspect ratio, the influence of the hole cavity on the incident beam and the confinement of the generated ablation products can lead to significant changes in the ablation progress. To study the drilling behavior in the depth of the material an in-situ observation of the evolution of the hole shape is necessary. Since this is not feasible for non-transparent samples, common approaches use breakthrough-time measurements [8], post processing of the sample with cut-and-polish techniques [9, 10], or optical coherence tomography [11, 12]. These methods either do not offer a time resolved measurement or only give access to limited information, e.g., the depth. Alternatively, drilling in semitransparent or transparent samples (e.g., ceramics or diamond) enables a direct observation of the hole formation [13, 14], but this is based on partial or nonlinear absorption and might therefore be different from highly absorbing materials like metals.

In our experiments, we used transmission imaging of a silicon sample, which is transparent for the illumination but opaque for the drilling radiation (1030 nm), to image a silhouette of the hole during the drilling process. This in-situ measurement enables us to follow the time-dependent evolution of the hole depth and longitudinal section throughout the whole progress in drilling. Therefore, the observations can reveal stochastical behavior, which is not possible with commonly used post-processing investigation methods.

S. Döring (✉) · S. Richter · A. Tünnermann · S. Nolte
Institute of Applied Physics, Friedrich-Schiller-University, Max-Wien-Platz 1, 07743 Jena, Germany
e-mail: sven.doering@uni-jena.de

A. Tünnermann · S. Nolte
Fraunhofer Institute for Applied Optics and Precision Engineering, Albert-Einstein-Strasse 7, 07745 Jena, Germany

A detailed description of the imaging setup can be found in [15]. Due to the similarity of the ablation behavior, observations in silicon can serve as a model system for the laser drilling of metals and other solids [16]. We investigate the influence of the process parameters pulse energy and fluence on the drilling behavior in the depth of the material. On the one hand, we perform a qualitative analysis of the hole shape and on the other hand we examine quantitatively the variation in time of the hole depth and sectional area as well as the maximum achievable depth.

2 Experimental setup

For our study, we performed percussion drilling using an ultrashort pulse laser (Trumpf TruMicro 5050) at a wavelength of 1030 nm and a pulse duration of 8 ps (FWHM). The system provides pulse energies of up to 125 µJ at repetition rates up to 400 kHz. To realize real time observation with a standard CCD camera, the repetition rate for drilling was set to 50 Hz. The beam was circularly polarized and focused to the sample surface by means of a plano-convex lens. The sample position is fixed with respect to the beam during drilling, implying the focus to be stationary on the sample's surface. We applied two approaches to realize different fluences on the sample surface. In the first place, we varied the pulse energy of the laser with the integrated electro-optic modulator. On the other hand, changing the spot size results in different fluences for the same pulse energy. We used lenses with focal lengths from 25 mm to 150 mm for this purpose. The actual spot size d_0 for each lens was measured by the technique described in [17]. The fluence F for pulses with energy E_P and a Gaussian beam with $1/e^2$-diameter d_0 was calculated by

$$F = \frac{8E_\mathrm{P}}{\pi d_0^2}. \tag{1}$$

Table 1 summarizes the beam diameters d_0 and the maximum achievable fluences F_max for all lenses in use. In the experiment, the actually applied fluences were in the range of 1 to 150 J/cm^2. Due to the percussion drilling geometry, the resulting hole diameter corresponds to the spot size.

Table 1 Spot size and maximum achievable fluence for each lens used in the experiments

Lens	d_0 (µm)	F_max (J/cm^2)
$f = 25$ mm	10.4 ± 0.5	294 ± 26
$f = 50$ mm	15.6 ± 0.3	130 ± 6
$f = 75$ mm	20.4 ± 0.7	76 ± 5
$f = 100$ mm	27.8 ± 0.3	41 ± 1
$f = 150$ mm	37.8 ± 0.6	22 ± 1

3 Evolution of the hole shape

Figure 1 shows the evolution of the longitudinal section of a hole during the percussion drilling process for various fluences. Each row represents one and the same hole for different numbers of applied pulses. A lens with focal length $f = 100$ mm was focused to the sample surface which is located at the top of each image. Please note the change in scaling from Fig. 1(b) to (c).

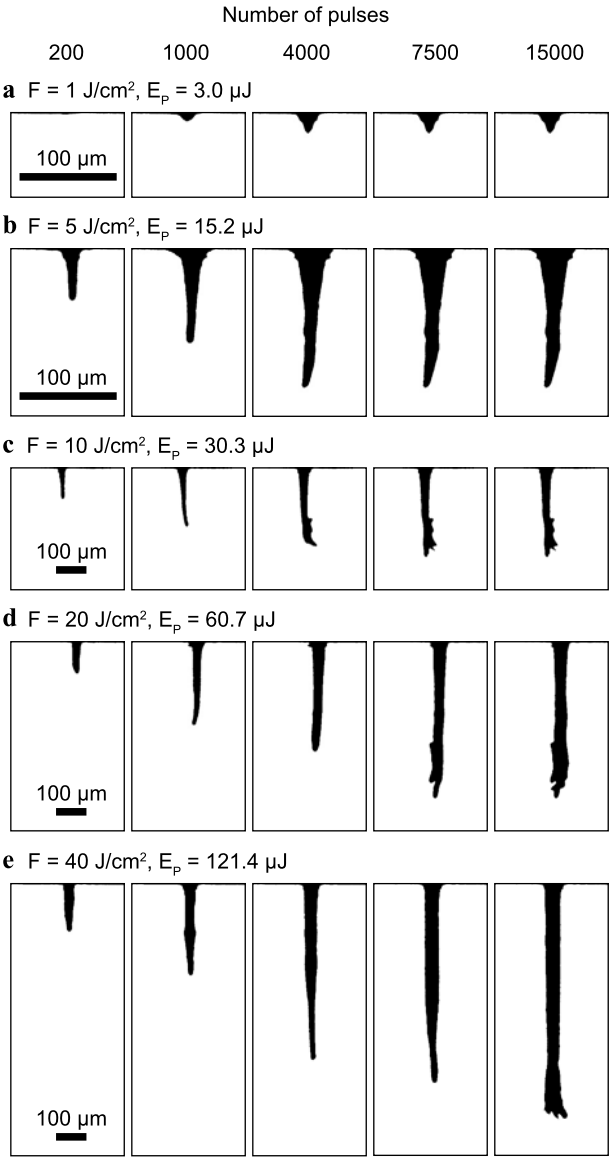

Fig. 1 Images of the longitudinal section of the hole during the percussion drilling process. For each fluence, the evolution of one hole is shown at various timesteps (numbers of pulses). See text for a detailed description

For a low fluence of $F = 1$ J/cm^2 (the measured threshold fluence for ablation for our pulse duration and wavelength is (0.26 ± 0.04) J/cm^2); see Fig. 1(a), no complete capillary is formed. The drilling process stops at approximately $N = 4000$ pulses, when a shallow deepening with v-shaped longitudinal section is formed. This stop in the drilling progress can be attributed to the increase of the effective irradiated area which results in a decrease of the applied fluence below threshold. We show this result for completeness, but concentrate on deep holes with a clearly formed capillary in the following.

At a fluence of $F = 5$ J/cm^2; see Fig. 1(b), the excavation of a hole capillary is observable during the first $N = 200$ pulses. Here, the hole has an ideal longitudinal section with respect to the percussion drilling conditions with a Gaussian shaped beam. This leads to a funnel shaped entrance and a tapered borehole. By the following pulses, the depth of the hole increases and its diameter is enlarged. From $N = 1000$ pulses on, the hole shows a small change in the drilling direction to the left side of the image. At $N = 4000$ pulses, forward drilling is completely stopped, while the hole diameter still increases until $N = 7500$ pulses, when no further change in the hole shape is experienced.

For an increased fluence of $F = 10$ J/cm^2, according to Fig. 1(c), the first part of the drilling process is comparable to $F = 5$ J/cm^2, which is the formation of the capillary and the further increase in depth with a change in the drilling direction at $N = 1000$ pulses. For this example, the bending happens to the right side. In addition, we observed a predominant transversal growth until $N = 4000$ pulses, leading to an increase of the diameter and formation of bulges and additional cavities along the sidewalls, especially in the lower part of the hole. This behavior can be attributed to internal reflections of the beam within the capillary. Other possible reasons are for instance the enhanced abrasive effect of the generated particles and plasma due to the confinement within the capillary. Deflection of the beam is also possible by scattering or absorption due to ablation products which may still remain in the hole when subsequent pulses arrive [19], although this seems improbable for the long pulse separation times used in our experiments. At the end of the drilling process at $N = 7500$ pulses, multiple hole ends are visible. These hole ends have been formed consecutively, which means that at first one ending is excavated and after its finish, another one occurred.

Higher fluences like $F = 20$ J/cm^2 and $F = 40$ J/cm^2 (see Figs. 1(d) and (e), respectively) show the same general behavior, including the deviations from the ideal shape, especially in the lower part of the hole as well as the formation of multiple ends. In these cases, ablation takes place for up to $N = 15000$ pulses. Noteworthy is the lower extend of deviations from the ideal hole shape for higher fluences/pulse energies. In comparison, only the lowest 20% of the hole are affected by imperfections in Fig. 1(e), while this portion is nearly 50% in case of $F = 10$ J/cm^2, Fig. 1(c). In addition, a more cylindrical upper part of the hole with decreased taper is formed at higher fluences. Small imperfections like the bulge in the middle of the hole at $N = 1000$ pulses in Fig. 1(e) vanish when the overall hole diameter increases until the end of the drilling process. Deviations in the drilling direction at the tip of the hole also emerge in a less distinctive way. The drawback, on the other hand, is the increased average hole diameter due to the higher fluence.

4 Development of hole depth and section area

For a further analysis of the drilling process, we measured the maximum depth and area of the longitudinal section for each timestep captured by the in-situ observation setup. Since this technique allows to observe the development of each single hole, we are able to follow the evolution of these quantities directly. Figure 2 shows a typical example for deep drilling at a fluence of $F = 10$ J/cm^2 with a lens of focal length $f = 100$ mm. For all other process parameters under investigation, which lead to deep drilling, we observed similar characteristics, while the absolute values of depth, longitudinal section and the number of pulses change. Therefore, the depth and the section area are normalized to their maximum values at the end of the drilling process (in this case at $N = 10\,000$ pulses). Please note the nonlinear scale of the abscissa for better visualization.

From this diagram three different phases of the drilling process can be distinguished, similar to [13, 14, 18]. The corresponding images of the hole shape can be seen in Fig. 1(c). Phase 1, from the start of the drilling to approximately $N = 200$ pulses, is characterized by a high ablation

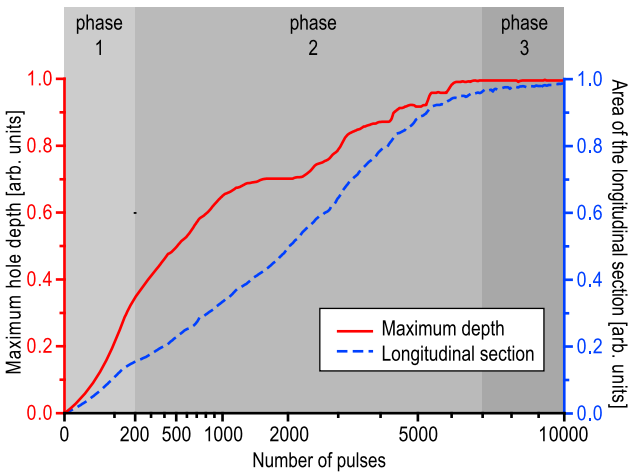

Fig. 2 Typical evolution of hole depth and longitudinal section area with the number of applied pulses during percussion drilling. Please note the nonlinear scaling of the abscissa. See text for a detailed description

rate. At the end of this phase already 30% of the final depth is reached. The hole has an ideal form for the percussion drilling conditions. We observed a nearly constant number of pulses (200 to 300) in the first drilling phase for all different process parameters used in the experiments.

Phase 2 ranges from approximately $N = 200$ to $N = 7000$ pulses. Note that the total number of pulses in this phase varies statistically from hole to hole, even if the same process parameters are applied. In this phase, the growth rate of the hole depth and volume is strongly reduced. The hole shape deviates from the ideal form. Bulges and cavities grow in transversal direction, the forward drilling direction can change and even multiple hole ends can occur. Therefore, the increase in depth happens stepwise. This observation is in agreement with in-situ depth profiling during drilling of semitransparent materials [13] and metals, realized by optical coherence tomography [11, 12].

In contrast to the evolution of the depth, the area of the longitudinal section, which can be assumed as a first-order approximation for the hole volume, shows a continuous increase. This means ablation takes place during the complete drilling process, but is not always directed in a forward direction. The plateaus in the development of the hole depth in Fig. 2 correspond to intermediate periods with predominant transverse growth. The onset of bulge formation changes statistically and can start from the beginning of phase 2, although drilling still happens primarily in forward direction.

At the end of phase 2, the hole depth reaches its final value, while the section area or volume of the hole is approximately 95%. Therefore, the hole volume increases in phase 3, but the depth remains constant. The growth in volume is mainly caused by an enlargement of the hole diameter due to erosion of the hole walls by the wings of the Gaussian beam profile [20]. Simultaneously, the formation of additional hole ends beneath the maximum depth may occur.

To evaluate the reproducibility of the drilling process, we repeated the process several times under constant conditions. Figure 3 shows the results using an $f = 100$ mm focal length lens at a fluence of $F = 10\,\mathrm{J/cm^2}$. In Fig. 3(a), $N = 200$ pulses have been applied, corresponding to the end of the first drilling phase. In this case, all holes show the same, ideal shape without any deviations in the form of bulges or a bending of the hole. The depth of these holes is also nearly identical and shows only minor differences. No further process control was used; the ablation process inherently provides the reproducible drilling behavior. Therefore, the drilling conditions in phase 1 are practicable for blind hole drilling.

In contrast, the growth of the holes in phase 2 of the drilling process is irregular. This results in different shapes of the holes, especially their lower parts, after e.g. $N = 3000$ pulses, see Fig. 3(b). The formation of bulges and additional cavities in the depth as well as the bending of the hole direction seem to be statistical processes, which can occur in any direction. Furthermore, the maximum depth achieved is also different for each hole, varying within approximately 15%. Nevertheless, the upper part of the holes at $N = 3000$ pulses is of comparable shape with ideal form at a length of at least 100 µm for these parameters. Therefore, the drilling conditions in phase 2 can be used for through hole drilling, in which the process parameters fluence/pulse energy and pulse-number can be optimized to suppress deviations in shape according to the workpiece thickness while reaching a higher depth than stopping the drilling after phase 1.

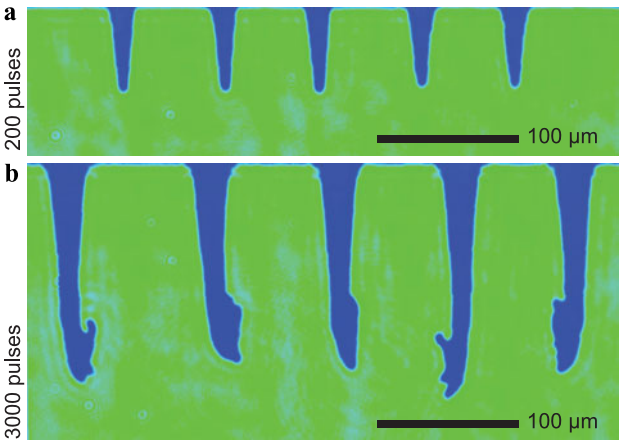

Fig. 3 The hole shape and depth generated after $N = 200$ pulses is highly reproducible and shows the ideal form for percussion drilling (**a**). The irregular drilling behavior in the following leads to different hole shapes after $N = 3000$ pulses (**b**)

5 Effect of fluence and pulse energy

To investigate the role of pulse energy and fluence on the drilling behavior, we performed a quantitative analysis of the maximum achievable hole depth in dependence of these quantities. Figure 4 shows the maximum achievable hole depth as a function of the applied fluence. For each specific lens, the depth rises when the fluence is increased, but each lens shows a different trend. For a constant fluence, the maximum achievable depth increases with the focal length used, which implies an accordingly increasing spot size and, therefore, a higher pulse energy. See, for example, the data points for $F = 20\ \mathrm{J/cm^2}$. Here, the maximum achievable depth increases from ca. 200 µm for $f = 50$ mm to ca. 780 µm for $f = 150$ mm by almost a factor of 4.

In Fig. 5, we replotted the measurement data of Fig. 4 as a function of pulse energy. In this picture, the depth increases with pulse energy, but this is largely independent from the lens used and the respective spot size. Hence, the achievable maximum depth is chiefly determined by the pulse energy and largely independent of the applied fluence. This behavior is in contrast to the conditions at the surface, where the

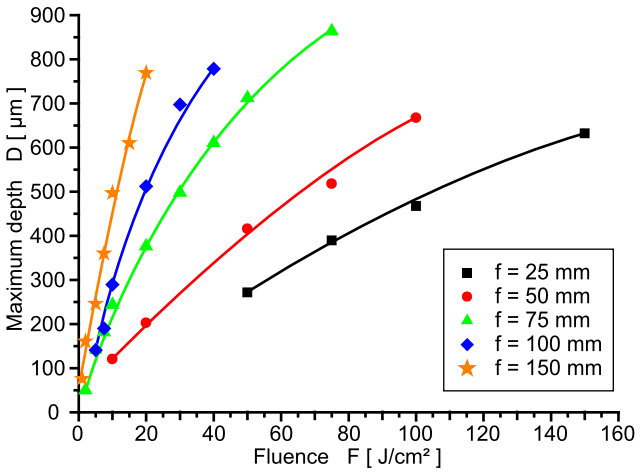

Fig. 4 The achievable hole depth depends on the applied fluence as well as the focusing conditions (lens used). The lines are a guide to the eye

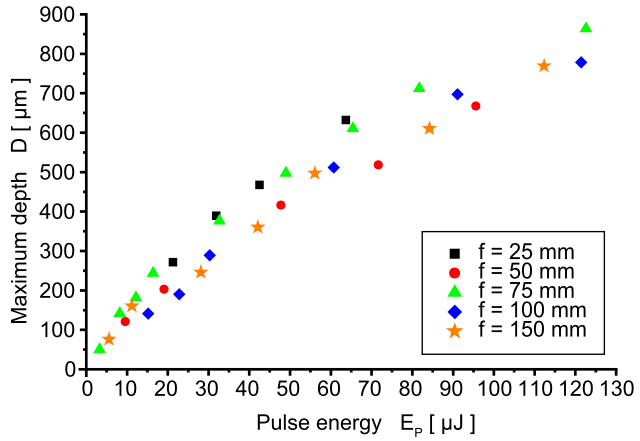

Fig. 5 The maximum achievable hole depth is mainly governed by the applied pulse energy, irrespective of the irradiated spot size or corresponding fluence

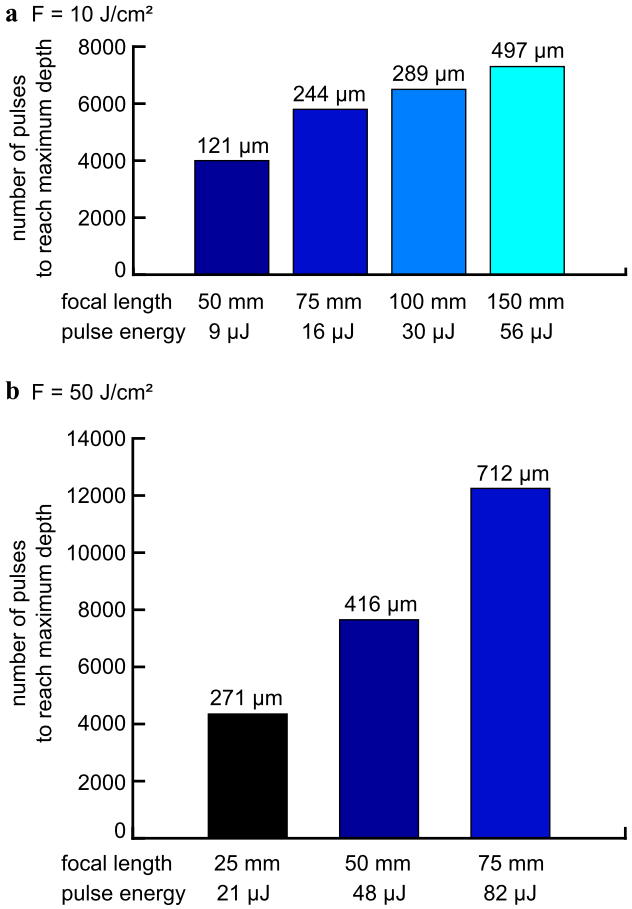

Fig. 6 The number of pulses to reach the final hole depth increases with focal length of the lens used and the applied fluence

fluence is the primary parameter, which determines the ablation rate (for example, the average ablation rate for ultrashort pulse ablation is in the order of several nanometers to about one micrometer per pulse and increases according to the applied fluence; see, e.g., [4] for details).

The maximum achievable drilling depth also shows a slight saturation with increasing fluence or pulse energy; see diagrams in Figs. 4 and 5. This means the energy available for ablation is decreased with increasing depth, which is in agreement with previous observations [9, 18, 21]. It is most likely that this is due to the same reasons as for the reduction of the drilling rate. These are the enlarged irradiated surface within the hole and, therefore, the reduced effective fluence as well as the enhanced heat conduction, furthermore the shielding by ablation particles and plasma within the capillary and the change in material expulsion due to the high aspect ratio of the hole [19].

In addition, attention should be paid to the absolute number of pulses necessary to reach the final depth of a hole (end of phase 2). This number varies according to process parameters fluence, focal length, and pulse energy used. Figure 6(a) shows examples for the number of pulses applied until the final depth was reached for a constant fluence of $F = 10$ J/cm^2. Here, a larger focal length leads to an increased number of pulses to finish forward drilling, which cannot be fully explained when assuming a fluence dependent ablation rate. For the increased focal length, the applied pulse energy has also increased to maintain a constant fluence, leading to a larger depth of the holes (indicated on top of each bar). Therefore, the ablated volume in total is also enlarged, which requires a longer drilling process. For higher fluences (compare, e.g., Fig. 6(b)), the total number of pulses increases even further with increased maximum achievable depth of the holes. However, note that the pulse numbers given here underly statistical variations, which is typical for the drilling process in phase 2 as de-

scribed above. This also leads to the statistical spread of data points in Fig. 5.

6 Conclusion

In conclusion, we have investigated the temporal evolution of the hole shape in percussion drilling with ultrashort laser pulses by direct observation of the drilling progress in silicon. Our observations showed at first the formation of an ideally shaped hole with high reproducibility. In a second phase, intermediate periods of predominant transversal growth can be observed, which lead to a stepwise increase in depth accompanied by deviations from the ideal hole shape in the form of bulges, changes in the drilling direction, and finally the formation of multiple hole ends. After the stop of forward drilling, the hole volume still increases by an enlargement of the hole diameter. For the deep drilling with ultrashort laser pulses, the maximum hole depth is chiefly governed by the pulse energy but largely independent from the irradiated spot size and the corresponding fluence at the surface. Therefore, it is advantageous to use high pulse energies to obtain the deepest possible holes. Nevertheless, one should consider the possible formation of cavities and bulges, which can be larger than the hole diameter determined by the spot size on the surface. These deviations from the ideal hole shape can be avoided by limiting the number of applied pulses to phase 1 of the drilling process. Since most of the imperfections are located in the lower part of the hole, the upper part can be used for drilling through holes with larger number of pulses, which allows to drill through a larger thickness.

Acknowledgements We acknowledge financial support from the Freistaat Thüringen (Grant No. 2007 FE 9020), the European Fund for Regional Development (EFRE), the Deutsche Forschungsgemeinschaft (DFG), and the Fraunhofer-Gesellschaft. Sören Richter acknowledges the Hans L. Merkle Stiftung for support.

References

1. D. Breitling, A. Ruf, F. Dausinger, Proc. SPIE **5339**, 49 (2004)
2. S. Preuss, A. Demchuk, M. Stuke, Appl. Phys. A **61**, 33 (1995)
3. B.N. Chichkov, C. Momma, S. Nolte, F. von Alvensleben, A. Tünnermann, Appl. Phys. A **63**, 109 (1996)
4. S. Nolte, C. Momma, H. Jacobs, A. Tünnermann, B.N. Chichkov, B. Wellegehausen, H. Welling, J. Opt. Soc. Am. B **14**, 2716 (1997)
5. S. Amoruso, B. Toftmann, J. Schou, R. Velotta, X. Wang, Thin Solid Films **453–454**, 562 (2004)
6. J. König, S. Nolte, A. Tünnermann, Opt. Express **13**, 10597 (2005)
7. S. Amoruso, R. Bruzzese, C. Pagano, X. Wang, Appl. Phys. A **89**, 1017 (2007)
8. A. Ancona, S. Döring, C. Jauregui, F. Röser, J. Limpert, S. Nolte, A. Tünnermann, Opt. Lett. **34**, 3304 (2009)
9. S. Bruneau, J. Hermann, G. Dumitru, M. Sentis, E. Axente, Appl. Surf. Sci. **248**, 299 (2005)
10. A. Michalowski, D. Walter, F. Dausinger, T. Graf, J. Laser Micro/Nanoeng. **3**, 211 (2008)
11. P.J.L. Webster, M.S. Muller, J.M. Fraser, Opt. Express **15**, 14967 (2007)
12. P.J.L. Webster, J.X.Z. Yu, B.Y.C. Leung, M.D. Anderson, V.X.D. Yang, J.M. Fraser, Opt. Lett. **35**, 646 (2010)
13. T. Abeln, J. Radtke, F. Dausinger, Proc. ICALEO **88**, 195 (1999)
14. T.V. Kononenko, V.I. Konov, S.V. Garnov, S.M. Klimentov, F. Dausinger, Laser Phys. **11**, 343 (2001)
15. S. Döring, S. Richter, S. Nolte, A. Tünnermann, Opt. Express **18**, 20395 (2010)
16. E. Coyne, J. Magee, P. Mannion, G. O'Connor, Proc. SPIE **4876**, 487 (2003)
17. J.M. Liu, Opt. Lett. **7**, 196 (1982)
18. A. Ruf, P. Berger, F. Dausinger, H. Hügel, J. Phys. D **34**, 2918 (2001)
19. F. Dausinger, F. Lichtner, H. Lubatschowski, *Femtosecond Technology for Technical and Medical Applications* (Springer, Berlin/Heidelberg, 2004)
20. C.S. Nielsen, P. Balling, J. Appl. Phys. **99**, 093101 (2006)
21. A.E. Wynne, B.C. Stuart, Appl. Phys. A **76**, 373 (2003)